ARMA 20–1990

Thermally-induced breakouts: insights from true-triaxial tests with acoustic emission monitoring

Trzeciak, M., Sone, H., Bate, C.E. and Wang, H.
University of Wisconsin-Madison, Madison, Wisconsin, USA

ABSTRACT: Borehole breakouts are used to constrain the magnitude of maximum horizontal stress. However, when the borehole wall strength is higher than the in situ tangential stress, borehole wall failure does not develop. Additional compressive stress can be induced by heating borehole walls. To validate this concept experimentally, we conducted room-temperature and elevated temperature true-triaxial tests on Berea sandstone and Niagaran dolomite samples. We used acoustic emission sensors to capture the onset of breakout development, and we measured the temperature close to borehole wall to assess the magnitude of induced thermal hoop stress. The test results show that within a specific rock type, the breakouts develop in similar manner in room-temperature and elevated-temperature tests. Therefore, the maximum horizontal stress can be constrained from the following dataset: critical tangential stress at which breakout develops, minimum horizontal stress, elastic and thermal properties, and temperature change at the borehole wall.

1. INTRODUCTION

Knowledge of in situ stress is crucial for many geological engineering applications including borehole stability analysis or hydraulic fracturing design. The stress tensor is commonly analyzed in principal directions assuming the direction of gravity is one of them. In such conditions stress description consists of finding the magnitudes of the vertical stress σ_v, the minimum horizontal stress σ_h, the maximum horizontal stress σ_H and the azimuth of horizontal stresses. In the current study, we focus on maximum horizontal stress magnitude assessment and we investigate thermally induced borehole breakouts to constrain it.

Compressive failure of the wellbore wall, i.e. breakout, develops when the circumferential stress $\sigma_{\theta\theta}$ at the borehole wall is higher than the rock strength. If the rock strength and the minimum horizontal stress magnitude are known, widths of breakouts provide important constraints on the magnitude of maximum horizontal stress. However, no breakouts occur when the rock strength is too high, which limits the information available to constrain stress. In such case, additional compressive circumferential stress may be induced by increasing the borehole wall temperature, leading to formation of thermally-induced breakouts. To test the feasibility of the method, we performed a series of laboratory tests where thermal breakouts were induced experimentally in a true-triaxial apparatus with fully controlled stress boundary conditions.

2. DESCRIPTION OF THE SAMPLES

We conducted laboratory tests using two rock types with different mechanical characteristics: Berea sandstone (BS), and Niagaran dolomite (ND). Both rock types are homogeneous and isotropic. BS is characterized by high porosity (23%) and low strength (55 MPa UCS – uniaxial compressive strength) while ND has low porosity (4%) and high strength (280 MPa UCS). Rock blocks with dimension of 5.5"x5.5"x8" were prepared from each rock type with 0.75" diameter boreholes predrilled at the center of the blocks.

3. EXPERIMENTAL SETTING

3.1. True-triaxial test setup

The true-triaxial apparatus used to induce borehole breakouts consists of a loading frame, which applies the vertical stress, and a cylindrical chamber with two pairs of hydraulic pistons that are used to apply the horizontal stresses (Fig. 1). The pistons are driven by two separate pressure intensifiers, which allows the independent application of the horizontal stresses.

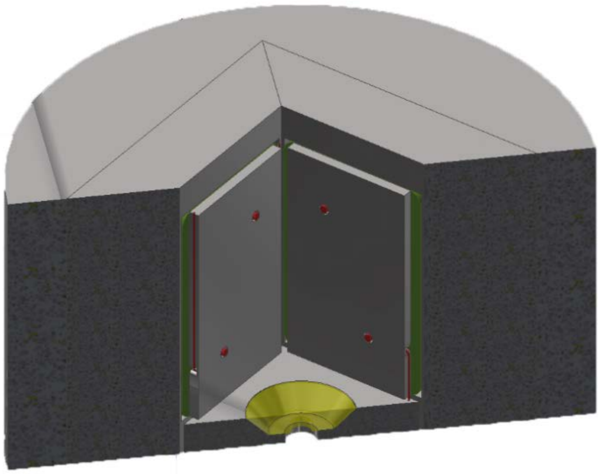

Fig. 1. Cross-section through true-triaxial cylindrical chamber with hydraulic pistons which apply the horizontal stresses.

The procedure for room-temperature true-triaxial tests was as follows: first, the hydraulic pistons and the loading frame were brought to contact with the rock sample. Next, all three principal stresses were increased simultaneously at a loading rate of 0.1 MPa per second to reach the intended minimum horizontal stress and vertical stress magnitude. After reaching the target stress values, the maximum horizontal stress, σ_H, was increased until the breakout formed, at loading rate 0.1 MPa per second. After the formation of the breakout the sample was unloaded, at 0.2MPa per second.

In elevated-temperature tests, the first stages were the same, but then the maximum horizontal stress was increased to magnitudes below the critical magnitude required to create a breakout found in the room-temperature tests. Additional compression necessary to induce compressive wellbore failure was induced by heating the borehole. We used a 7.5” long, 0.5” diameter cartridge heater to heat the borehole wall.

3.2. *Acoustic emission data acquisition*

Eight acoustic emission sensors contacted the rock sample directly during the true-triaxial tests and recorded acoustic emission events. Additionally, active pulsing was performed in 60 s intervals to measure velocities. The acquisition frequency spectrum of the sensors we used was 0.1-0.8 MHz, with maximum sensitivity between 0.2 and 0.3 MHz. Sensor configuration is depicted in Fig. 2. The data have been recorded using Vallen AMSY-6 acoustic emission acquisition system, and later processed in Matlab.

3.3. *Borehole camera recording*

During room-temperature true-triaxial tests we additionally deployed a borehole camera inside the borehole, to record the visual appearance of the borehole wall during formation and development of breakout structures.

3.4. *Temperature data acquisition*

During elevated-temperature tests, the temperature was measured by twelve thermocouples deployed in 0.16” diameter boreholes drilled from the corners of the block towards the main borehole wall. The thermocouples were installed at approximately 0.1”, 0.2”, 0.4” and 0.8” from the borehole wall, at three heights, 3.25”, 4”, and 4.75” (Fig. 2).

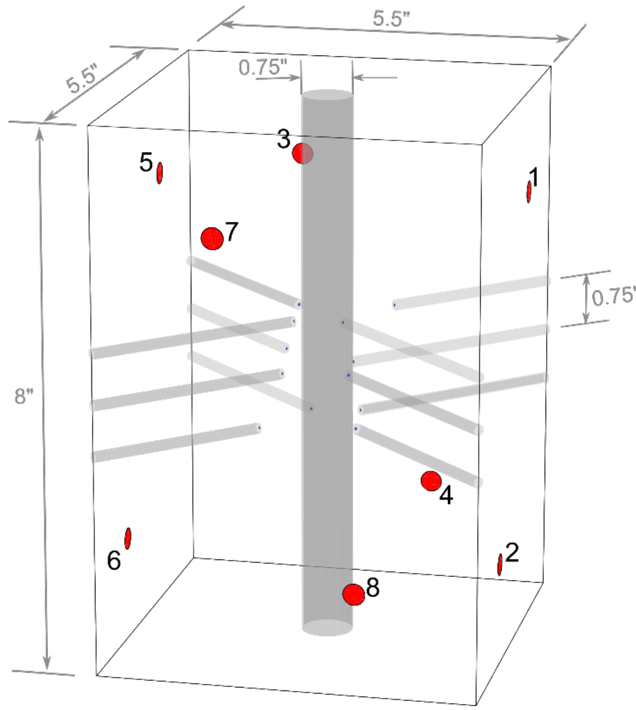

Fig. 2. Sample dimensions, acoustic emission sensors configuration (red circles), and thermocouple positions (blue dots).

4. EXPERIMENTAL DATA

4.1. *Uniaxial compressive strength, porosity and thermal expansion*

Before the main true-triaxial experiments, we conducted preliminary tests to constrain the uniaxial compressive strength, elastic constants, density, porosity and thermal expansion of the rocks used in the experiments. The results obtained from these tests are summarized in Table 1.

Table 1. Strength, elastic parameters, density, porosity and thermal expansion of Berea sandstone and Niagaran dolomite.

property	Berea sandstone	Niagaran dolomite
UCS [MPa]	55±4[1]	281.8±1.3
E [GPa]	22.0±4.0[1]	68.2±0.7
ν [-]	0.17±0.04[1]	0.25±0.03
density [kg/m^3]	2046±3	2722±5
porosity [%]	22.8±0.00	4.1±0.15
linear thermal expansion [m/mK]	$1.48 \cdot 10^{-5}$	$1.51 \cdot 10^{-5}$

[1] data from (Hart & Wang, 1995).

4.2. Room-temperature true-triaxial tests

The main goal of the room-temperature tests was to measure the critical tangential stress at which the breakout develops. We call this critical stress value the borehole compressive strength, or BCS, in order to distinguish from the UCS of the rocks. This distinction was made since we find that the BCS is typically larger than the UCS possibly due to scale and geometry effects.

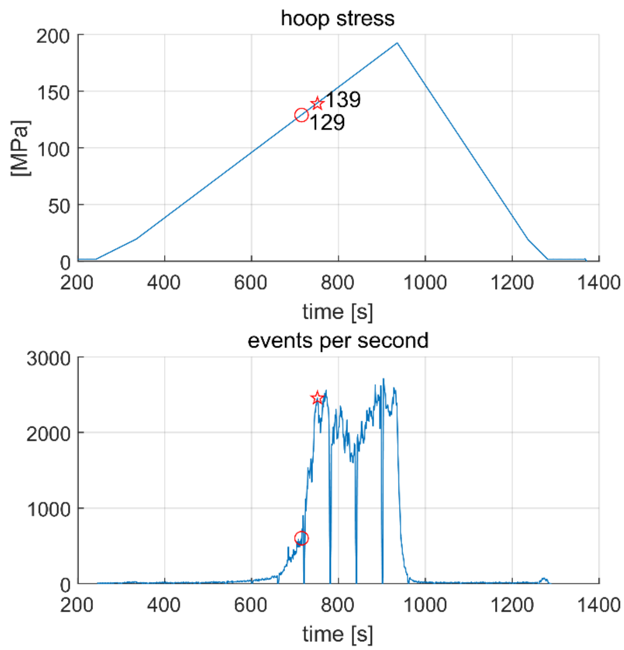

Fig. 3. Room-temperature true-triaxial test results for Berea sandstone sample; top – hoop stress from the Kirsch solution [MPa], bottom – number of recorded acoustic emission events per second. Circle denotes onset of increased AE activity. Star denotes visible failure from the borehole camera.

The onset of borehole wall failure was captured by increase in acoustic emission rate, and by borehole camera recording.

The tests were performed on dry rock samples, with no pore pressure and no mud pressure. Thus, we calculated the maximum tangential stress (hoop stress) at the borehole wall from the Kirsch solution (Zoback, 2007):

$$\sigma_{\theta\theta} = 3\sigma_H - \sigma_h \tag{1}$$

The test on Berea sandstone started with loading the sample hydrostatically to $\sigma_H = \sigma_h = \sigma_v = 10$ MPa. Next, the maximum horizontal stress was increased to 70 MPa. Significant increase in acoustic emission activity was noted at σ_H=46.3 MPa and visible failure was recorded by the borehole camera at σ_H=49.7 MPa, which correspond to hoop stress equal to 129 and 139 MPa, respectively. The lower of these values is taken as the borehole compressive strength of the Berea sandstone. The test results are depicted in Fig. 3, with the BCS value indicated by red circle.

During the room-temperature experiment on Niagaran dolomite, we applied vertical stress σ_v=5 MPa, and σ_h=0 MPa. Then, the maximum horizontal stress was increased to 139 MPa, corresponding to 417 MPa hoop stress, where the stress capability of our system was reached and we could not continue loading. The breakout formation was recorded by the borehole camera 50 seconds after the loading stopped (red star in Fig. 2). Even though the main failure occurred after the loading stopped, acoustic emission rate data suggest earlier beginning of the failure process, at hoop stress equal to 370 MPa (red circle Fig. 2.)

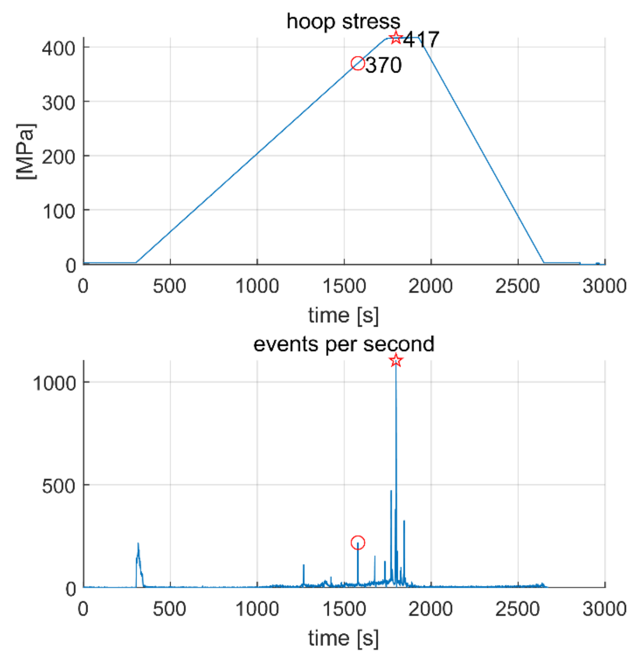

Fig. 4. Room-temperature true-triaxial test results for Niagaran dolomite sample; top – hoop stress [MPa], middle – number of recorded acoustic emission events per second. Circle denotes onset of increased AE activity. Star denotes visible failure from the borehole camera.

4.3. Elevated-temperature true-triaxial tests

In the elevated-temperature test the Berea sandstone sample was first loaded to $\sigma_v = 10$, $\sigma_h = 10$, and $\sigma_H = 25$ MPa, which corresponds to 65 MPa hoop stress. Then, the heater was turned on, and the borehole wall approached maximum temperature of approximately 220ºC. The test data is presented in Fig. 5.

The Niagaran dolomite sample was loaded to $\sigma_v = 5$, $\sigma_h = 5$, and $\sigma_H = 100$ MPa, which corresponds to hoop stress equal to 295 MPa. Next, heating started, and the borehole wall reached maximum temperature of approximately 170ºC. The test data is presented in Fig. 6.

5. EXPERIMENTAL DATA INTERPRETATION

5.1. *Experimental data overview*

Presented experimental data show that breakouts develop as a result of heating the borehole wall even when the in situ stresses are too low (or the strength of the rock is too high) to induce compressive wall failure. Additionally, comparing the room-temperature and elevated-temperature tests, we see similar acoustic emission activity in both test types. Berea sandstone produces large number of events, the breakout develops gradually as the hoop stress (both mechanical and thermal) increases. Conversely, breakout formation in Niagaran dolomite sample is localized and abrupt, and the number of acoustic emission events is low.

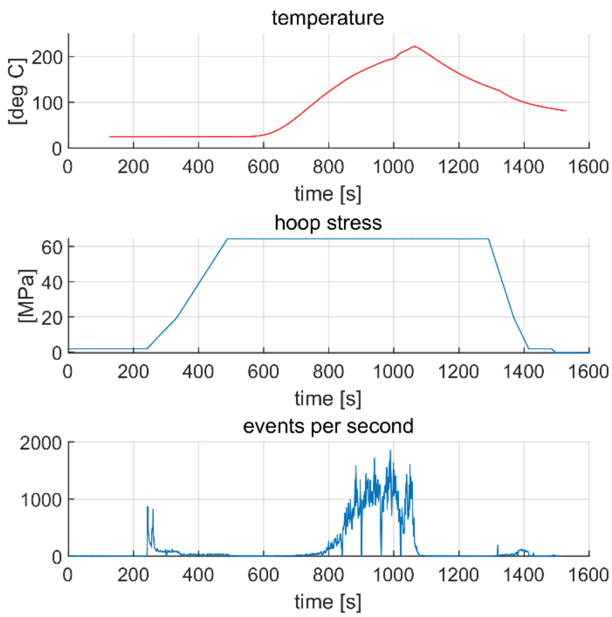

Fig. 5. Elevated-temperature true-triaxial test results for Berea sandstone sample; top – temperature data recorded by a thermocouple installed 0.1” from borehole wall, middle – hoop stress [MPa], bottom – number of recorded acoustic emission events per second.

5.2. *Thermally induced hoop stress*

The magnitude of thermally induced hoop stress on the borehole wall can be derived from elastic and geometrical analysis. Heating of a material induces expansion, described by the coefficient of linear thermal expansion. Thus, we can define linear thermal strain as:

$$\varepsilon_0^T = -\alpha \Delta T \qquad (2)$$

where α is the coefficient of linear thermal expansion, and ΔT is temperature change; minus sign follows from the positive compression convention. Then, from cylindrical form of Hooke’s law we can solve for thermal hoop stress:

$$\begin{bmatrix} \sigma_{rr}^T = 0 \\ \sigma_{\theta\theta}^T \\ \sigma_{zz}^T = 0 \end{bmatrix} = \begin{bmatrix} c_{11} & c_{12} & c_{12} \\ c_{12} & c_{11} & c_{12} \\ c_{12} & c_{12} & c_{11} \end{bmatrix} \begin{bmatrix} \varepsilon_{rr}^T = -\alpha\Delta T \\ \varepsilon_{\theta\theta}^T = 0 \\ \varepsilon_{zz}^T \neq 0 \end{bmatrix} \qquad (3)$$

where c_{ij} are components of the elastic stiffness matrix (assuming isotropy). The assumptions in Eq. (3) are:

- radial stress is zero, because borehole wall is a free surface,
- vertical thermal stress is zero,
- the hoop strain is zero (radial strain is infinitesimal thus the circumference change is negligible),
- there is nonzero thermal vertical strain.

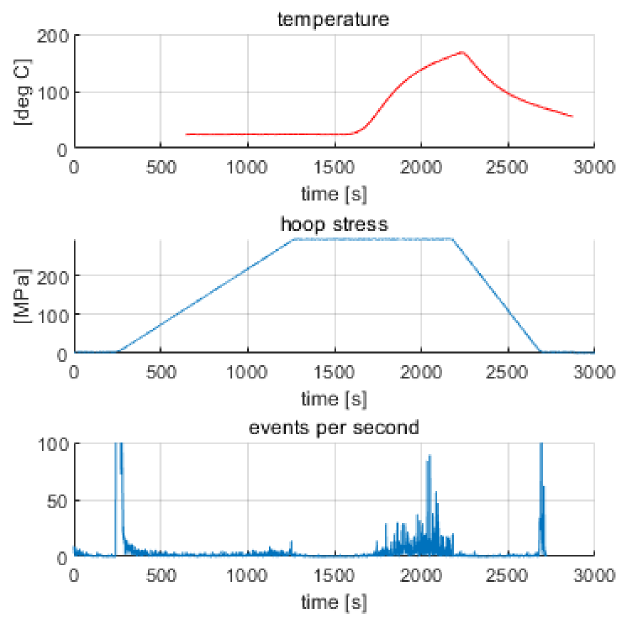

Fig. 6. Elevated-temperature true-triaxial test results for Niagaran dolomite sample; top – temperature profile recorded by thermocouple at depth 0.1” from borehole wall, middle – hoop stress [MPa], bottom – number of recorded acoustic emission events per second.

From the third equation in (3), we get the formula for vertical strain:

$$\varepsilon_{zz}^T = \frac{1-\nu}{\nu} \alpha \Delta T \qquad (4)$$

which is then inserted into second equation in (3) to get (Stephens and Voight, 1982, Jaeger et al. 2007):

$$\sigma_{\theta\theta}^T = \frac{\alpha E}{1-\nu} \Delta T \qquad (5)$$

where E is the Young’s modulus, and ν is the Poisson’s ratio.

Eq. (5) relies on simple geometric considerations, but it can be used as first-order approximation of the thermal stress.

5.3. *Maximum horizontal stress estimation*

Thermally induced breakouts can be used to estimate the maximum horizontal stress. Let's assume that we know the minimum horizontal stress, temperature at the borehole wall, borehole compressive strength, and we captured the moment of breakout formation. Then, the maximum horizontal stress can be calculated from:

$$\sigma_H = \frac{1}{3}\left[\sigma_{\theta\theta}^{cr} + \sigma_h - \frac{\alpha E}{1-\nu}\Delta T\right] \qquad (6)$$

where $\sigma_{\theta\theta}^{cr}$ is the critical hoop stress (BCS), other symbols are as in Eq. (2).

For Berea sandstone, we assume that the BCS equals 129 MPa (Fig. 3), and the onset of thermal breakout formation was captured at ΔT = 115ºC (red circle at Fig. 7). Using elastic and thermal parameters from Table 1, Eq. (6) gives σ_H = 31.3 MPa. The applied maximum horizontal stress in the analyzed experiment was 25 MPa.

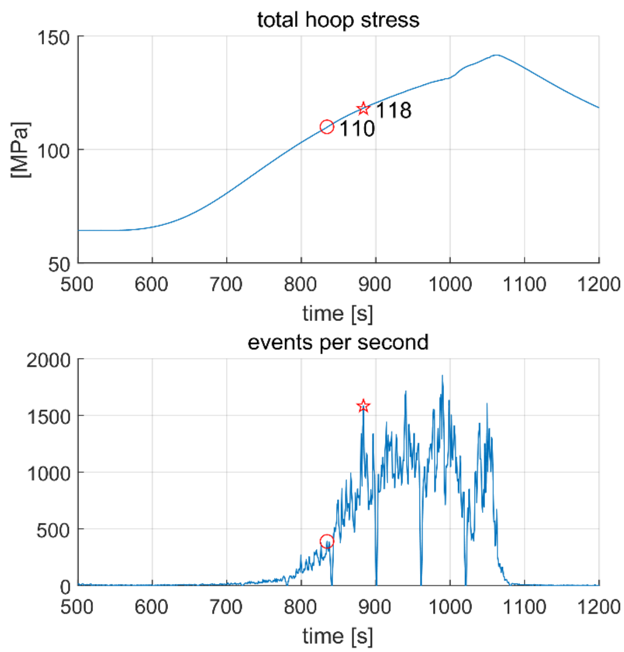

Fig. 7. Comparison of total hoop stress (mechanical and thermal) with acoustic emission rate for Berea sandstone sample. Circle denotes onset of increased AE activity. Star denotes visible failure from the borehole camera.

For the Niagaran dolomite sample, we assume BCS equal to 370 MPa (Fig. 4), and onset of thermal breakout formation at ΔT=58ºC (red circle in Fig. 4). Then, Eq. (3) gives σ_H = 98.5 MPa. In this experiment, the maximum horizontal stress was set to 95 MPa. If we use 417 MPa as the BCS (red start on Fig. 8), then the estimated maximum horizontal stress equals 114 MPa.

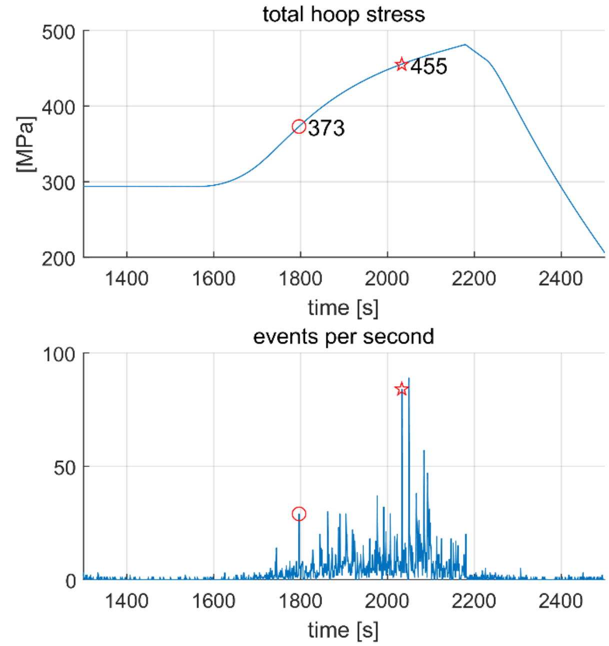

Fig. 8. Comparison of total hoop stress (mechanical and thermal) with acoustic emission rate for Niagaran dolomite sample. Circle denotes onset of increased AE activity. Star denotes visible failure from the borehole camera.

There are several sources of uncertainty in maximum horizontal stress assessment using the thermal breakout method. Borehole wall temperature measurement, and elastic parameter estimation seem to be minor problems compared to reliable assessment of borehole strength. Identifying the timing of the breakout occurrence from AE data, as well as the very definition of breakout occurrence also needs to be examined further.

6. CONCLUSIONS

Laboratory true-triaxial tests and data analysis led us to the following conclusions:

- thermally induced breakouts can be used to estimate maximum horizontal stress magnitudes in boreholes where stresses are too low for the breakouts to occur at in situ temperature,
- maximum horizontal stress assessment uncertainty is mostly influenced by borehole strength input and methods used to identify the timing of breakout formation.

ACKNOWLEDGMENTS

This material was based upon work supported by the U.S. Department of Energy, National Energy Technology Laboratory under Award Number DE-FE0031688 with RESPEC.

REFERENCES

1. Hart, D.J., & Wang, H.F. (1995). Laboratory measurements of a complete set of poroelastic moduli for Berea sandstone and Indiana limestone. *J. geophys. res.*, *100*(B9), 17,741-17-751.
2. Jaeger, J.C., Cook, N.G.W., & Zimmermann, R.W. (2007). Fundamental of rock mechanics. Wiley Blackwell.
3. Stephens, G., & Voight, B. (1982). Hydraulic fracturing theory for conditions of thermal stress. *Int. J. Rock Mech.* & *Min. Sci. & Geomech. Abstr.*, *19*(6), 279–284.
4. Zoback, M.D., (2007). Reservoir Geomechanics. Cambridge University Press.